RIGA TECHNICAL UNIVERSITY
Faculty of Civil Engineering
Institute of Building Production

Artūrs Lukašenoks
Doctoral Student of the Study Programme "Civil Engineering"

COMPOSITE FIBRE DEVELOPMENT AND INVESTIGATION OF PULL-OUT BEHAVIOUR IN CONCRETES WITH VARIOUS STRENGTH

Summary of the Doctoral Thesis

Scientific supervisor
Professor Dr. sc. ing.
ANDREJS KRASŅIKOVS

RTU Press
Riga 2018

Lukašenoks A. Composite fibre development and investigation of pull-out behaviour in concretes with various strength. Summary of the Doctoral Thesis. Riga: RTU Press, 2018. 31 p.

Published in accordance with the decision of the Promotion Council RTU P-03 of 22 June 2018, Minutes No. 2018-2.

ISBN 978-9934-22-128-6 (print)
ISBN 978-9934-22-129-3 (pdf)

DOCTORAL THESIS PROPOSED TO RIGA TECHNICAL UNIVERSITY FOR THE PROMOTION TO THE SCIENTIFIC DEGREE OF DOCTOR OF ENGINEERING SCIENCES

To be granted the scientific degree of Doctor of Engineering Sciences, the present Doctoral Thesis has been submitted for the defence at the open meeting of RTU Promotion Council on September 14, 2018 at the Faculty of Civil Engineering of Riga Technical University, 1 Kaļķu Street, Room 119, Riga, Latvia.

OFFICIAL REVIEWERS

Lead Researcher Dr. sc. ing. Jānis Andersons
Institute of Polymer Mechanics, the University of Latvia

Professor Dr. sc. ing. Janis Varna
Luleå University of Technology, Sweden

Head of Laboratory Dr. sc. ing. Valentin Antonovič
Vilnius Gediminas Technical University, Lithuania

DECLARATION OF ACADEMIC INTEGRITY

I hereby declare that the Doctoral Thesis submitted for the review to Riga Technical University for the promotion to the scientific degree of Doctor of Engineering Sciences is my own. I confirm that this Doctoral Thesis had not been submitted to any other university for the promotion to a scientific degree.

Artūrs Lukašenoks ……. (signature)
Date: ……

The Doctoral Thesis has been written in English. It consists of Introduction; 5 Chapters; Conclusion; 141 figures; 44 tables; 2 appendices; the total number of pages is 153. The Bibliography contains 155 titles.

TABLE OF CONTENTS

1. GENERAL DESCRIPTION OF THE RESEARCH

1.1. Introduction

Fibre reinforced concrete (FRC) is a composite material – concrete matrix reinforced with discrete fibres. Conventionally it was considered that fibres are oriented chaotically and uniformly throughout the concrete matrix volume. However, several types of research have shown that uniform and chaotic fibre orientation is not possible due to several reasons – mould wall effect, concrete flow, concrete compaction [1]–[4]. Fibres in the concrete volume, when located near the mould surface, stack up along the surface. Concrete flow during the pumping or transportation process aligns fibres along the flow direction, but the orientation is mixed up immediately after entering the mould or standing concrete volume. Concrete placing and compaction significantly influence fibre positioning in volume. Fibre two-dimensional orientation can be achieved without special measures if the layer of placement is slightly smaller than fibre length. Fibre compaction with the vibrating tables and poker vibrators induces concrete flow and therefore fibre orientation. Studies of fibre orientation and distribution have been done using image processing, inductive tests, X-ray and THz electromagnetic waves [5]–[7]. Many researchers have concluded that fibre location and orientation cannot be controlled during the concrete casting process [8]. This conclusion is valid if the fibre has to be positioned (located and oriented) very precisely. Experience in the construction industry shows that high requirements to the concrete matrix properties, fresh concrete control have to be ensured to create the minimum confidence for the fibre location and orientation. Stability of the fresh concrete mix is a necessary condition, on the other hand, good concrete workability is required to reduce concrete compaction in the moulds. Uncontrolled compaction and vibrations result in unknown fibre layout.

FRC can be very attractive in production and construction process. Significant amount of labour work can be transferred from reinforcement production (meshes, bent shapes), transportation (lifting, carrying), installing (cage tying, welding) to the process point of discrete fibre introduction and mixing in the concrete volume. In conventional cast-in-situ construction, reinforcement works are the second most significant part of man-hours consumed after formworks [9]. Fibre reinforced concrete placing, compaction and processing are mechanised in higher grade compared to reinforcement works.

Steel fibre type is most commonly used as disperse reinforcement for structural applications with different geometrical shapes and size [10]. Fibre shapes are straight or deformed to increase pull-out resistance (with hooks on the ends, undulated). Polymer fibres have much lower stiffness and strength compared to steel, and they mainly are used to reduce the shrinkage cracking in structural elements [11]. The properties of polymer fibres have been continuously improved. The recent technological development of a wide variety of polymer fibres has enabled new opportunities for the development of micro-fibre reinforced cementitious composites for use in overlays for pavements, floor toppings and structural applications [12]–[16].

Other types of synthetic fibres such as glass, basalt, aramid, and carbon have high strength, stiffness, and low specific gravity. These fibres are chemically stable in severe environmental conditions. Unfortunately, due to the small diameter of glass, basalt aramid, and carbon fibres, it is difficult to introduce them into concrete. The fibres form clews and rolls when mixed into the concrete with conventional techniques (drum, pan, twin-shaft or planetary mixers). The problem with fibre incorporation in the mix becomes more pronounced with high fibre dosages. All mentioned fibres are split or torn into shorter pieces when mixed with concrete in high-speed mixers [17].

In recent years, investigations in composite materials have significantly contributed to the manufacturing technology of composite and fibre materials, which has reduced their cost and increased their use. Very few information on composite fibres is found. Unidirectional basalt fibre – polymer matrix composite elements with a rectilinear geometry and round smooth cross sections (Minibar^{TM}) now are available on the market (similar product to composite fibres). Basalt Minibar fibres are recommended for use in high volume fractions (1.5-–3 %) in order to achieve tangible results [18], [19]. Long carbon fibres impregnated with epoxy resin are used to increase the impact blast resistance of concrete plates for military applications [20]– [22].

Previously mentioned studies of fibre reinforced concrete and fibre pull-out focus on only one concrete matrix type or compressive strength [23]–[25]. Current research presents a study on the strength level of three different concrete matrices. Each matrix strength level represents a group of concretes that are used in the concrete and construction industry. Low strength concrete in the study represents the group of concretes with a compressive strength range 30–40 MPa used mostly for pavements, floors, and foundations. Medium strength concrete in the range of 50–75 MPa represents a group of concretes used widely in precast industry for walls, pre-stressed beams, plates, bridge decks, and roads. High strength concrete in the range of 90–125 MPa is used relatively less in comparison to the previous two groups and is used in precast industry for mock-up façade elements, heavy loaded beams, balconies, thin plates and sheets.

1.2. Objectives of the research

The objectives were to develop a new type of composite fibres for concrete disperse reinforcing, to investigate single fibre pull-out behaviour and fibre failure mechanisms in concretes with three compressive strength levels, and to study fibre performance in concrete tested in flexure.

1.3. Tasks of the research

To achieve the objectives of the research, the following tasks were set:

- to develop fibres with high strength, diameter in range 0.9–2.7 mm, and of several shapes and surface structures;
- to develop fine-grained concrete with three concrete compressive strengths of approximately 40 MPa, 75 MPa and 120 MPa;

- to manufacture fibres and samples in order to investigate single fibre pull-out behaviour in concrete matrices with mechanical testing;
- to introduce composite fibres in concrete and test fibre reinforced concrete behaviour in flexure.

1.4. The methodology of the research

The Introduction of the Doctoral thesis presents a literature review on fibres, fibre reinforced concrete and concrete technology. Scientific publications were used to formulate the objective of the research and the tasks. Four tasks were set to achieve the objectives of the study.

The first task of the study was to develop the fibres. To execute this task, adequate fibre manufacturing technique was found for manufacturing of each fibre type: smooth, rough surface fibre, braided fibre and hybrid fibre. Manufacturing technique had to meet fibre surface, geometry and quality requirements.

Development of concrete matrices with three different strength levels was the second task of the study. Sets of constituents were selected to iterate the concrete mixes and test the fresh, hardened concrete properties. Only appropriate mix designs that meet the necessary strength levels are presented in the study. Standard testing methods for determination of concrete matrix properties (slump flow, compressive strength, strength development, shrinkage) were used.

The third task of the research was accomplished by manufacturing and testing composite fibre and single fibre pull-out samples in order to find the relation between force and pull-out displacement with different parameters (concrete matrix strength, fibre embedment depth, fibre configuration angle, fibre surface and shape). Each fibre configuration had at least seven samples. Single fibre pull-out tests were carried out with testing machine Zwick Z150 (mounted additional load dynamometer 1000 N), and the displacement was measured using non-contact measuring device – video extensometer Messphysik (resolution 1 μm). The results were processed using Microsoft Excel and MATLAB software. From the obtained force-displacement curves and data, average relationships for embedment depth, angle configuration and matrix strength were found.

The final task of the research was completed by manufacturing large amounts of composite fibres, preparing samples in standard beam moulds as well as by testing. Prior to the fibre introduction the concrete was tested to meet the requirements for fresh concrete properties and final strength. Beam samples were tested in four-point bending and the obtained results were processed. Load bearing capacity of the beams containing composite fibres was analysed and compared with the known steel fibres. From the obtained results, force-deflection average relationship was found for different parameters (influence of fibre count in crack plane, concrete matrix strength, and composite fibre surface properties).

1.5. Scientific novelty

A new type of composite glass, carbon and hybrid fibres are presented in this Doctoral thesis. There is very few research on the composite fibres, but there were not found methodical investigation on fibre pull-out from the concrete matrix. Pull-out tests were carried out systematically in concrete matrices with three different compressive strength levels (approximately 40 MPa, 75 MPa and 120 MPa). Compressive strength levels were developed to represent three different large groups of concretes that are used in the construction industry. Marginal surface properties (smooth and rough), as well as fibre shapes (straight and braided), were manufactured during the development of the new fibres.

1.6. Structure of the Dissertation thesis

The structure of the Doctoral Thesis is presented in Fig. 1.1. Background information and the scientific problem of the Thesis is formulated in Introduction. Chapters 2–6 are dedicated to carrying out of the tasks of the Thesis. Major conclusions are summarized and presented in Conclusions.

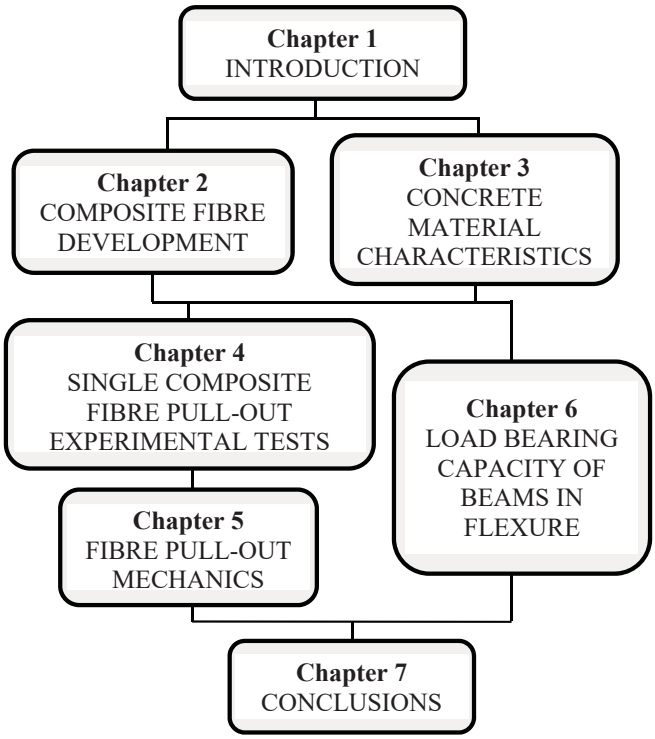

Fig. 1.1. Structure of the Doctoral Thesis.

1.7. List of conferences and publications

Results of the Thesis that have been presented at international conferences and published in conference proceedings (indexed in international databases):

1. Šahmenko, G., Krasnikovs, A., Lukašenoks, A., Eiduks, M. Ultra high performance concrete reinforced with short steel and carbon fibers. Paper presented at the 10th International Scientific Practical Conference "Environment. Technology. Resources", 18–20 June 2015, Rezekne, Latvia, 193–199. doi:10.17770/etr2015vol1.196 Retrieved from www.scopus.com (*author's contribution 45%)*
2. Lukasenoks, A., Macanovskis, A., Krasnikovs, A., Lapsa, V. Composite fiber pull-out in concretes with various strengths. Paper presented at the 15th International Scientific Conference "Engineering for Rural Development", 25–27 May 2016, Jelgava, Latvia, 1417-1423. Retrieved from www.scopus.com *(author's contribution 90%)*
3. Lukasenoks, A., Macanovskis, A., Krasnikovs, A. Matrix strength influence on composite fibre reinforced concrete behaviour in flexure and single fibre pull-out. Paper presented at the 17th International Scientific Conference Engineering for Rural Development, 23–25 May 2018, Jelgava, Latvia, 1513–1520. DOI: 10.22616/ERDev2018.17.N365 Retrieved from www.scopus.com *(author's contribution 90%)*
4. Lukasenoks, A., Macanovskis, A., Krasnikovs, A. Composite carbon fibre embedment depth and angle configuration influence on single fibre pull-out from concrete. Paper presented at the 17th International Scientific Conference Engineering for Rural Development, 23–25 May 2018, Jelgava, Latvia, 1507–1512. DOI: 10.22616/ERDev2018.17.N364 Retrieved from www.scopus.com (*author's contribution 90%)*

Results of the Thesis presented at international conferences and published in conference proceedings:

5. Šahmenko, G., Krasņikovs, A., Stonys, R., Lukašenoks, A., Eiduks, M. Nano-Modified Fibre Reinforced Concrete. In: 3rd All-Russia (International) Conference "Concrete and Reiforced Concrete – Glance at Future", Moscow, 12–16 May, 2014, Moscow: 2014, 230–238. ISBN 9785726408095. *(author's contribution 45%)*

Results of the Thesis presented at the conferences and accepted for publication in proceedings:

6. Lukasenoks, A., Krasnikovs, A., Macanovskis, A., Kononova, O., Lapsa, V. Short Composite Fibres For Concrete Disperse Reinforcement. Paper presented at Euromech Colloquium 582 "Short Fibre Reinforced Cementitious Composites and Ceramics", 20–22 March 2017, Tallinn, Estonia *(author's contribution 85%)*

Results of the Thesis submitted for publication in the scientific journal American Concrete Institute (ACI) Materials Journal (accepted for publication):

7. Macanovskis, A., Lukasenoks, A., Krasnikovs, A., Stonys, R., Lusis, V. (2018) Composite fibers in concretes with various strengths. ACI Materials Journal *(author's contribution 75%)*

2. CONTENT OF THE DOCTORAL THESIS

This thesis consists of an introduction, five chapters and conclusions. The Introduction presents an extensive background to subjects covered in the following chapters.

In **Chapter 2** composite fibre development is discussed: fibre filament material selection, manufacturing techniques, quality control and general geometry, and surface properties.

The objectives of composite fibre development are to develop fibres with high strength, different fibre geometry and improved fibre surface in order to increase fibre resistance to pull-out, as well as to develop a technology for producing composite fibres in laboratory conditions as well as technology for fibre industrial manufacturing. Development of composite fibres is necessary because there are no commercially available products with the desired diameter and length. Composite fibres in this work are considered as glass, carbon or combined fibre filaments impregnated with epoxy resin. The following key requirements for composite fibres were set: high fibre strength, and suitable fibre surface for good grip with the concrete matrix. Since high strength for fibres was required, glass and carbon fibre materials were chosen. Several steps were iterated to produce smooth, rough, wavy surface of composite fibres.

Fibre manufacturing consists of fibre filaments and matrix (epoxy resin) transformation into macro fibres. Fibre filaments are prepared before the manufacturing of macro fibres, a necessary number of filaments is separated from the main thread, or yarn, or placed together and pre-stored. For the braided fibres, where it is necessary, yarns are interlaced together to form a fibre filament braid. The main stages of composite fibre manufacturing are shown in Fig. 2.1.

Fig. 2.1. Raw fibre transformation stages into the composite fibre.

Three types of composite fibres were developed and denominated with capital letters CF (carbon fibres), GF (glass fibres) and CG/GC (hybrid fibres). Each fibre type has a subtype which is numbered. Composite carbon fibres have three subtypes: CF1 (smooth surface), CF2 (rough surface) and CF3 (braided fibre). Smooth and rough fibres have three different diameters, which were obtained using a distinctive number of filaments (24k, 16k and 8k).

Smooth composite carbon fibres CF1, CF1-A and CF1-B are shown in Fig. 2.2 and schematic representation is in Fig. 2.5, which shows straight smooth fibres with three diameters.

Fig. 2.2. Composite carbon fibres: CF1, CF1-A and CF1-B (from the left).

Rough surface composite carbon fibres CF2, CF2-A and CF2-B are shown in Fig. 2.3 and schematic representation is in Fig. 2.5, which shows straight fibre with rough surface (three diameters).

Fig. 2.3. Composite carbon fibres: CF2, CF2-A and CF2-B (from the left).

Braided composite carbon fibre CF3 is shown in Fig. 2.4. Schematic representation in Fig. 2.4 shows undulated fibre, which is obtained by interlacing fibre filaments.

Fig. 2.4. Braided composite carbon fibre CF3.

Fig. 2.5. Schematic representation of composite carbon fibres: CF1, CF1-A, CF1-B (smooth); CF2, CF2-A, CF2-B (rough), and CF3 (interlaced) from the left.

Composite glass fibres have five subtypes: GF1 (smooth surface, uneven shape), GF2 (smooth surface) and GF3 (rough surface), GF4 (interlaced fibre with 14 braids) and GF5 (interlaced fibre with seven braids). All composite glass fibres have the same number of filaments but a different manufacturing technique that results in distinctive shape and surface.

Three composite glass fibres GF1, GF2 and GF3 are shown in Fig. 2.6 and schematic representation is in Fig. 2.8.

Fig. 2.6. Composite glass fibres GF1, GF2 and GF3 (from the left).

Two composite glass fibres GF4 and GF5 are shown in Fig. 2.7.

Fig. 2.7. Composite glass fibres: GF4 and GF5 (from the left).

Schematic representation is shown in Fig. 2.8, which shows that fibres are straight with undulated surface and have a different number of interlaced braids.

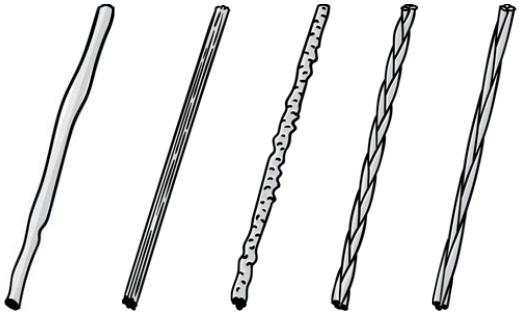

Fig. 2.8. Schematic representation of braided composite glass fibres: GF1, GF2 GF3, GF4, and GF5 (from the left).

Hybrid fibres have two subtypes; both have undulated surface, which was created by interlacing carbon and glass fibre filaments. The main distinction between the two fibres is the core and circumjacent fibre material. Hybrid fibre CG1 has carbon fibre filaments in the core and glass fibre interlaced around. Fibre GC1 has glass fibre filaments in the core and carbon fibre interlaced around.

Fibres CG1 and GC1 are shown in Fig. 2.9 and the schematic representation is in Fig. 2.10, which shows that fibres are straight with undulated surface and have a different core and circumjacent fibre material.

Fig. 2.9. Hybrid composite fibres: CG1(on the left) and GC1 (on the right).

Fig. 2.10. Schematic representation of hybrid composite fibres: CG1 and GC1 (from the left).

A summary with an average diameter and specific gravity is given in Table 2.1 for in total 14 developed composite fibres. All fibres are 50 mm long with a diameter in the range of 0.89–2.76 mm. Fibres are grouped into three main groups: composite carbon fibres (CF), composite glass fibres (GF), and hybrid fibres (CG/GC). Fibres have different shapes: uneven, straight and undulated. Fibre surface finish is normally smooth, but there is one composite glass fibre (GF3) and three composite carbon fibres (CF2, CF2-A and CF2-B) whose outer surface is improved with fine quartz sand grains, resulting in rough fibre surface (Latvian patent application P-16-101).

Table 2.1

Summary of Composite Glass, Carbon and Hybrid Fibre Properties

Fibre type	Labelling	Fibre geometry, surface	Diameter, mm	Specific gravity, kg/m^3
Carbon fibres	CF1	Straight, smooth	1.77	1129
	CF1-A	Straight, smooth	1.3	1291
	CF1-B	Straight, smooth	0.89	1569
	CF2	Straight, rough	2.1	1397
	CF2-A	Straight, rough	1.79	1330
	CF2-B	Straight, rough	1.57	1183
	CF3	Undulated, smooth	1.82	1101
Glass fibres	GF1	Uneven, smooth	2.18	1195
	GF2	Straight, smooth	1.52	1746
	GF3	Straight, rough	2.04	1507
	GF4	Undulated, smooth	1.88	1310
	GF5	Undulated, smooth	1.85	1270
Hybrid fibres	CG1	Undulated	2.6	–
	GC1	Undulated	2.76	–

Chapter 3 covers fine-grained concrete development with three concrete strengths: compressive strength from 40–120 MPa. The objectives of this chapter are to present materials for fine-grained concrete, which are developed in this research, and to test the methods for characterising concrete material properties in fresh and hardened stage. Concrete matrix compressive strength range of 40–120 MPa (M1–M3) is based on the current situation and development perspectives in the concrete and construction industry. In the construction industry, concrete with a compressive strength of 40 MPa is very popular for various applications (slabs on grade, walls, foundations). Concrete with a compressive strength of 70–75 MPa is considered as high strength concrete in the industry, and special measures (materials used, production technology, method of laying and curing) are required. Concrete with a compressive strength of 120 MPa is niche concrete product and its use is determined only by special measures, and in most cases, they differ from regular concrete production and

application significantly. Compositions (material combinations) of concrete matrices M1, M2 and M3 are presented in Table 2.2.

Table 2.2

Concrete Mixture Proportions (M1, M2 and M3)

Materials	Density, kg/m^3	M1, kg/m^3	M2, kg/m^3	M3, kg/m^3
Cement CEM I 52,5R	3130	800	550	400
Water	1000	200	300	300
Sand 0–1 mm	2650	1100	1200	1400
Silica fume	2220	133.3	50	0
Quartz powder 0–120 μm	2650	66.5	250	250
Superplasticizer	1070	25	6.5	3
w/c ratio	–	0.25	0.55	0.75
w/b ratio	–	0.21	0.5	–
Paste volume, l/m^3	–	540.7	592.6	522.1

Before casting single fibre pull-out concrete samples, a flow test by the ASTM C1437 was performed. Fig. 2.11 shows the brass cone mould used during this test and spread (on the right and in the middle). Tests were carried out to control workability. Consistency measurement results were in the range of 220–295 mm for all mixes.

Fig. 2.11. Concrete consistency measurements for concrete M1.

Fresh concrete properties were also measured according to EN 12350-8 (Slump-flow test) before casting beam moulds. Four measurements were made for each concrete (M1, M2, and M3). The testing process is shown in Fig. 2.11 (on the right), and the results are presented in Table 2.3. All three concrete matrices were flowable: measured slump flow was from 580–770 mm. Such good flowing abilities of the fresh concrete were designed intentionally, in order to fill narrow moulds and to increase ease of concrete placement.

Table 2.3

Concrete Mixture Consistency Measurements According to EN 12350-8

Concrete mixture	Flow diameter, mm	Standard deviation, mm	Consistency class	Fresh concrete density, kg/m^3
M1	768	32	SF3	2296
M2	743	33	SF2	2164
M3	580	28	SF1	2157

Concrete matrix type M1 has the highest average strength of f_c = 122.3 MPa, M2 has medium average strength of f_c = 74.86 MPa, and M3 has the lowest average strength of f_c = 41.84 MPa. Concrete compressive strength for M2 and M1 is about 1.8 times and 2.9 times higher than M3.

Concrete shrinkage was determined according to ASTM C157 "Test Method for Length Change of Hardened Hydraulic-Cement Mortar and Concrete". Sets of three concrete samples were prepared for each concrete matrix (M1, M2, and M3). Moulds for samples with size 75 mm x 75 mm x 275 mm were used. Samples were cast and demoulded after 23 ± 1 h, measured and stored in water. Samples were in water storage (23 ± 0.5 °C) for 14 days, samples from the 15th day were placed in air storage (RH 50 ± 4 %, 23 ± 2 °C). Concrete moisture content was determined by weighing samples at each length change measurement. Concrete matrices M2 and M3 are increasing in sample weight during first 14 days, contrary to concrete matrix M1 when all these samples were stored in water. M1 has a very low w/c ratio and high internal structure density. Shrinkage of concrete matrices from the 28th day is as follows: for M1– 130 με, for M2 – 426 με, and for M3 – 188 με.

Chapter 4 covers single fibre pull-out sample manufacturing and experimental programme, with details about the non-standardized testing method, sample size, fibre configurations and testing. In this chapter, a general comparison of fibre pull-out behaviour is made for all tested fibres (in total 14 fibres) at equal fibre configuration parameters. Fibre pull-out testing and investigation is important because it governs post cracking behaviour. Fibre pull-out (with high resistance) is the most optimal behaviour in fibre reinforced concrete.

Single fibre pull-out samples were manufactured and tested to investigate fibre behaviour and resistance to extraction from the concrete matrix. Fibre pull-out experiments were aimed to investigate different fibre and concrete parameter (strength, diameter, geometry and surface) influence on fibre performance as well as fibre pull-out and failure mechanisms.

Single fibre pull-out samples were manufactured in self-designed moulds for each concrete matrix (M1, M2, and M3) and fibre type. When mould design was considered, several objectives were set: high quality of samples (precise geometry, fibre alignment), ease of assembly, cleaning and disassembly of moulds, reusability (durability). Two concrete opposite parts were cast and plastic film was used to separate concrete; sample geometry is shown in Fig. 2.12. A small opening in the plastic film allowed composite fibre to connect two concrete pieces. Different mould sizes were used: Type A (40 mm × 60 mm × 30 mm) and Type B

(80 mm × 100 mm × 30 mm). The sample with two concrete parts was chosen to enable the testing of single fibre pull-out at a configured angle and to observe fibre pull-out from both sides of the concrete matrix, which is existing in real fibre reinforced concrete structure behaviour.

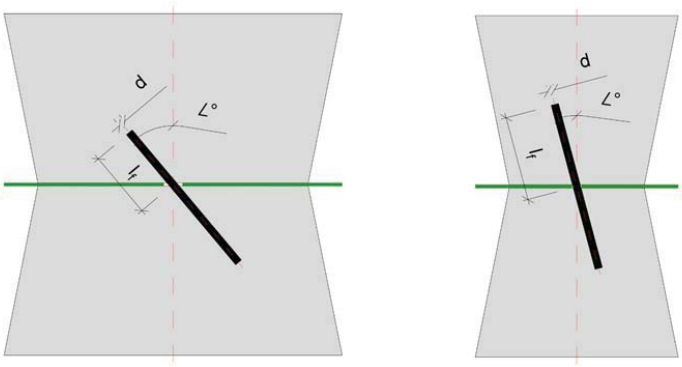

Fig. 2.12. Sample geometry sketch: Type A on the right, Type B on the left. Fibre configurations: depth l_f = 25, 20, 15, 10 and 5 mm; and angle ∠ = 0°, 15°, 30°, 45° and 60°.

Pull-out sample casting process consists of mould preparation (separator, fibre installation) and placing concrete into the mould. Concrete is placed in two stages. Concrete is mixed according to the procedure described in Chapter 3 and the consistency is tested. One part of the mould is filled with concrete completely and fibre is checked and adjusted if necessary (depth and angle as shown in Table 2.4). Samples with fibre configuration in angle and depth and casting process are presented in Fig. 2.13.

Fig. 2.13. Fibre configurations in depth (first and second on the left), moulds filling with concrete (on the right).

In this figure, the first picture on the left is composite glass fibre GF2 in mould Type B. The fibre is configured at a 45-degree angle and 20 mm in depth. One of the sample sides is already filled with concrete. The second picture from the left is composite carbon fibre CF1 in mould Type A. The fibre is configured at a 0-degree angle and 15 mm in depth. One of the sample sides is already filled completely with concrete, the filling process on the other side of the sample has been started. In the picture on the right the concrete filling process is shown for

composite carbon fibre CF3, configured at a 0-degree angle and 25 mm in depth. The concrete mix shown in the figure is very flowable and suitable for small concrete sample manufacturing. All manufactured single fibre pull-out samples were labelled with manufacturing date, fibre type, configuration parameters (fibre angle and depth) and concrete matrix. The samples were covered with plastic and stored in laboratory conditions for at least 24 h, then demoulded and cured. Sample demoulding was made carefully, all bolts were released and each plywood mould part was removed. A set of 7 samples was manufactured for each configuration and concrete matrix. The total amount of samples manufactured and tested was 1323.

Table 2.4

Single Fibre Pull-out Configuration Table (Embedment Depth, Angle and Sample Type) for Each Concrete M1, M2 and M3

Configuration angle / Embedment depth	Sample Type A – 0°	Sample Type A – 15°, 30°	Sample Type B – 45°, 60°
5 mm	CF1, CF1-A, CF1-B; CF2, CF2-A, CF2-B; CF3; SF1, SF2; GF2	-	-
10 mm	CF1, CF1-A, CF1-B; CF2, CF2-A, CF2-B; CF3; SF1, SF2; GF2	-	-
15 mm	CF1, CF1-A, CF1-B; CF2, CF2-A, CF2-B; CF3; SF1, SF2; GF2	CF2-B	CF2-B
20 mm	CF1, CF1-A, CF1-B; CF2, CF2-A, CF2-B; CF3; SF1, SF2; GF2	CF1, CF1-B, CF3 (only M3), GF2	CF1, CF1-B CF3 (only M3), GF2
25 mm	CF1, CF1-A, CF1-B; CF2, CF2-A, CF2-B; CF3; SF1, SF2; GF2; GF1, GF3, GF4, GF5 (only M3); CG1, GC1 (only M3)	-	-

Chapter 5 presents single fibre pull-out experimental findings (for 10 fibre types in 3 concrete matrices), a broad discussion is made on fibre pull-out and failure mechanisms, conclusions on further fibre development and use are made. The objectives of this chapter are to investigate single composite fibre pull-out mechanics and failure mechanisms in concrete matrices M1, M2, and M3 configured in different depth and angle. Due to fibre hand manufacturing process, fibres are not extremely uniform. Nevertheless, fibre failure modes are analysed and highest possible performance is being sought, that shows fibre potentioal if there would not be defects from hand manufacturing technique. Different fibre failure modes point out various fibre pull-out and fracture mechanisms, as well as flaws and defects in fibre manufacturing process. Ability to identify the most appropriate technological process for fibre fabrication will lead to new fibre development and opportunity to use as disperse reinforcement in concrete.

The chapter is organized and test results are discussed in eight subchapters: (1) Carbon micro-fibre and multi-walled carbon nanotube (MWCNT) influence on straight steel fibre pull-out behaviour; (2) Fibre embedment depth influence on pull-out; (3) Influence of fibre angle configuration on pull-out behaviour; (4) Concrete matrix strength influence on single fibre pull-out; (5) Smooth composite fibre diameter influence on single fibre pull-out; (6) Composite fibre shape and surface influence on single fibre pull-out; (7) Load rate influence on pull-out behaviour; (8) Fibre failure modes.

Carbon micro-fibre and multi-walled carbon nanotube (MWCNT) influence on straight steel fibre pull-out behaviour

Analysis of the pull-out curves and pictures made with SEM shows that MWCNT does not give significant improvement to the concrete matrix – fibre channel and the concrete matrix is cracked. Concrete matrix cracking is occurring due to steel fibre geometry stability and high elasticity modulus. Concrete matrix is shrinking around the fibre and cracks when strain limit is reached. From this, it can be concluded that reinforcing gradation level is not sufficient when only carbon microfibres and MWCNT are used in nano level. There is a huge gap between two reinforcing fibre sizes. Adding short carbon fibres (micro-fibres) in the concrete mix did not show a positive result on straight steel macro fibre pull-out behaviour. Experimental results confirmed that the highest effect on single steel fibre (embedment depth – 25 mm, configuration angle 0-degree, diameter – 0.79 mm) pull-out from concrete matrix can be obtained by having a high strength matrix with carbon nanotubes and micro and nano-sized admixture, such as silica fume. In fact, highest positive effect measured gives only approximately 8 % of peak pull-out force and 8 % of pull-out energy increase.

Fibre embedment depth influence on pull-out

Single fibre pull-out tests were made for two steel fibres (SF1, SF2), three composite carbon fibres (CF1, CF2, and CF3) and composite glass fibres (GF2). All mentioned fibre pull-out tests are consistently made in three concrete matrices M1, M2, and M3. The results for other fibre subtypes (CF1-A, CF1-B, CF2-A, and CF2-B) are presented in Appendix 1. Pull-out laws discussed in Chapter 5 reflect interrelationship inherent for similar fibres CF1-A, CF1-B, CF2-A, and CF2-B (same shape and surface, different diameter).

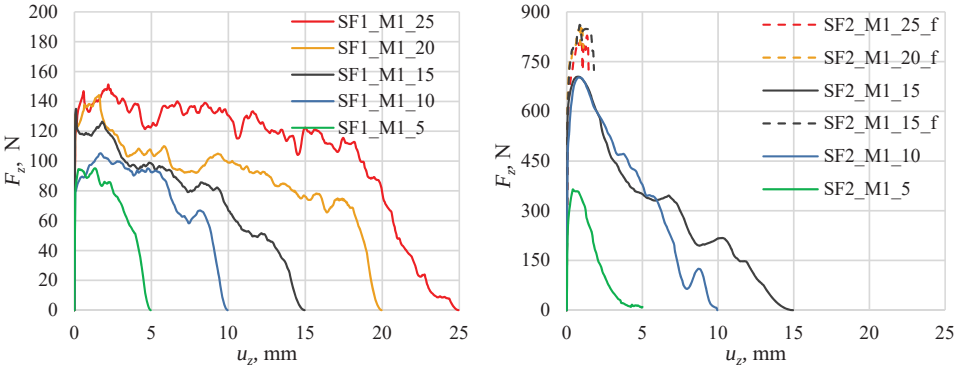

Fig. 2.14. Average single fibre pull-out behaviour curves for SF1 (on the left) and SF2 (on the right), configurations: embedded in depth 25, 20, 15, 10 and 5 mm. Concrete matrix M1.

All presented results are for fibre configuration: 5, 10, 15, 20, and 25 mm depth, 0-degree angle to pull-out force. The only examples of single fibre pull-out curves at different embedment depth are presented in the Summary of the Thesis. Steel fibre SF1, SF2 results with concrete matrix M1 are shown in Fig. 2.14.

Composite fibre CF1 and CF2 pull-out results in concrete matrix M1 are shown in Fig. 2.15.

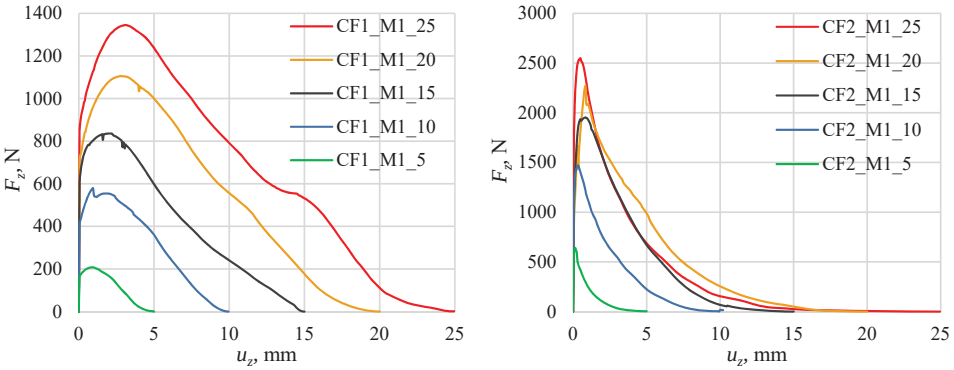

Fig. 2.15. Average single fibre pull-out behaviour curves for CF1 (on the left) and CF2 (on the right), configurations: embedded in depth 25, 20, 15, 10 and 5 mm. Concrete matrix M1.

Fibre peak pull-out forces from each fibre embedment depth were collected and plotted for three concrete matrices M1, M2, and M3. In Fig. 2.16 (on the left), it can be seen that there exists a linear relationship between straight smooth steel fibre (SF1) peak pull-out force and fibre configuration's embedment depth.

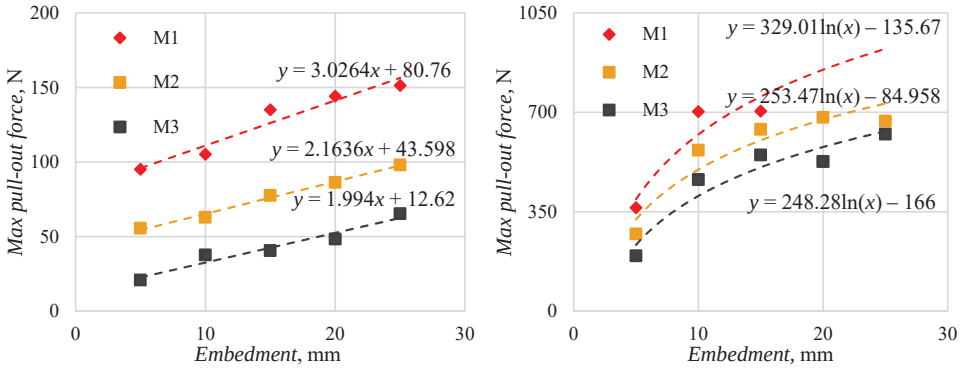

Fig. 2.16. Single smooth steel fibre SF1 (on the left) and corrugated SF2 (on the right) peak pull-out force depending on fibre embedment depth (5–25 mm) in three concrete matrices: M1, M2, and M3.

In Fig. 2.16 (on the right), it can be seen that there exists a logarithmic relationship between smooth undulated steel fibre (SF2) peak pull-out force and fibre configuration's embedment depth. However, pull-out force in concrete matrix M1 does not exceed 700 N due to the fibre tensile strength – fibre shape created too high anchorage and the fibre does not pull-out.

In Fig. 2.17 (on the left), it can be seen that there exists a linear relationship between the peak pull-out force of smooth carbon fibre (CF1) and embedment depth of fibre configuration.

Unlike the smooth SF1 fibre, carbon fibre (CF1) does not have parallel embedment-peak pull-out force relationship, on contrary – as the concrete matrix becomes stronger, fibre peak pull-out force is rising steeper with an increase of the depth of fibre configuration. Fibre pull-out peak force increase trendline is almost twice steeper for M2 compared with M3, and for M1 compared to M2.

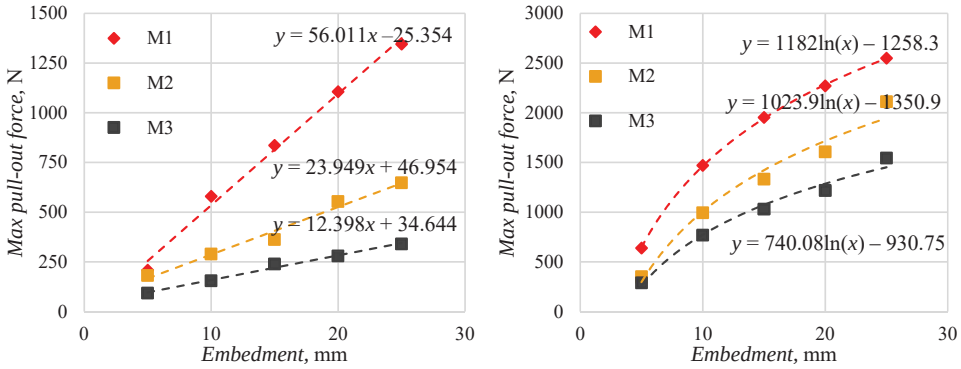

Fig. 2.17. Peak pull-out force of single composite fibre CF1 and CF2 (from the left) depending on fibre embedment depth (5–25 mm) in concrete matrices: M1, M2, and M3.

In Fig. 2.17 (on the right), it can be seen that there exists a logarithmic relationship between the peak pull-out force of rough surface carbon fibre (CF2) and embedment depth of fibre configuration. Average pull-out curves are less uniform and in force decrease phase overlaps with other fibre depth configurations. This is related to fibre surface, where the rough outer layer is created by adding fine sand grains to epoxy resin. Fibre surface roughness with grains is not perfectly uniform and the manufacturing process produces overconcentration of grains and defects in local fibre surface areas.

In Fig. 2.18, it can be seen that there exists a logarithmic relationship between the peak pull-out force of corrugated carbon fibre (CF3) and embedment depth of fibre configuration.

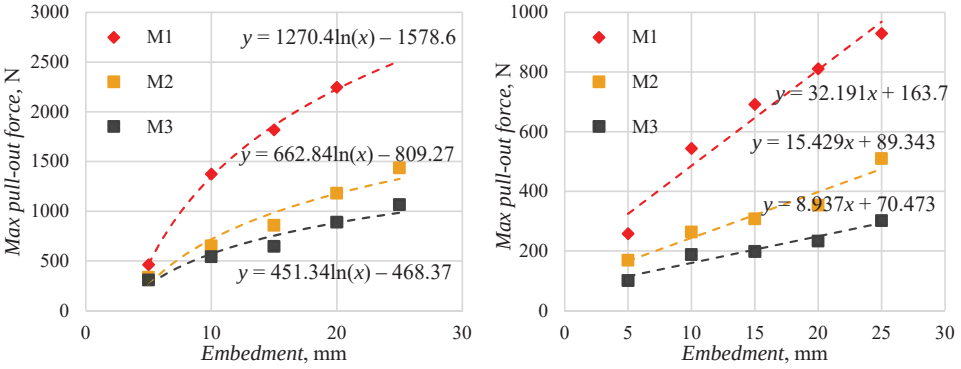

Fig. 2.18. Single composite fibre CF3 (on the left) and GF2 (on the right) peak pull-out force depending on fibre embedment depth (5–25 mm) in concrete matrices: M1, M2, and M3.

Carbon fibre (CF3) has similar significant pull-out peak force growth for M1 compared to M2 and M3 as smooth carbon fibre (CF1). This can be explained by fibre, epoxy layer and

concrete matrix pull-out mechanism. Both CF1 and CF3 have only thin epoxy layer on carbon fibre core unlike CF2, which has a significantly thicker epoxy layer with grains, which anchors fibre in the concrete matrix. CF1 and CF3 have similar interface failure mechanism between fibre and concrete.

From Fig. 2.18 (on the right), it can be seen that there exists a linear relationship between the peak pull-out force of smooth glass fibre (GF2) and embedment depth of fibre configuration.

Influence of fibre angle configuration on pull-out behaviour

Single fibre pull-out results (fibres configured at an angle) are presented for four composite fibres: CF1, CF1-B, CF2-B, and GF2. The fibres are configured at 5 different angles starting from 0 and incremented by 15 degrees – 0, 15, 30, 45, and 60. Tests with higher configuration angles were not carried out due to large inclination to crack surface. Smooth composite fibres CF1, CF1-B, and GF2 were embedded 20 mm deep in concrete, rough surface fibre GF2-B was embedded 15 mm deep. Embedment depth was reduced by 5 mm due to possible fibre pull-out failure.

Concrete matrix strength influence on single fibre pull-out

Composite fibre configuration was set at a 0-degree angle to pull-out force and 25 mm embedment depth to investigate concrete matrix strength influence on single fibre pull-out behaviour. Composite carbon fibres with smooth surface CF1, CF1-A, CF1-B and rough surface CF2, CF2-A, CF2-B as well as braided composite carbon fibre CF3 and smooth glass fibre GF2 were used to investigate concrete strength influence on pull-out.

Smooth composite fibre diameter influence on single fibre pull-out

Composite fibres with a smooth surface were selected, the configuration was set at a 0-degree angle to pull-out force and 25 mm embedment depth to investigate fibre diameter influence on single fibre pull-out behaviour. Composite carbon fibres with smooth surface CF1, CF1-A, CF1-B and composite glass fibre GF2 were used. The investigation was carried out with three concrete matrices M1, M2, and M3.

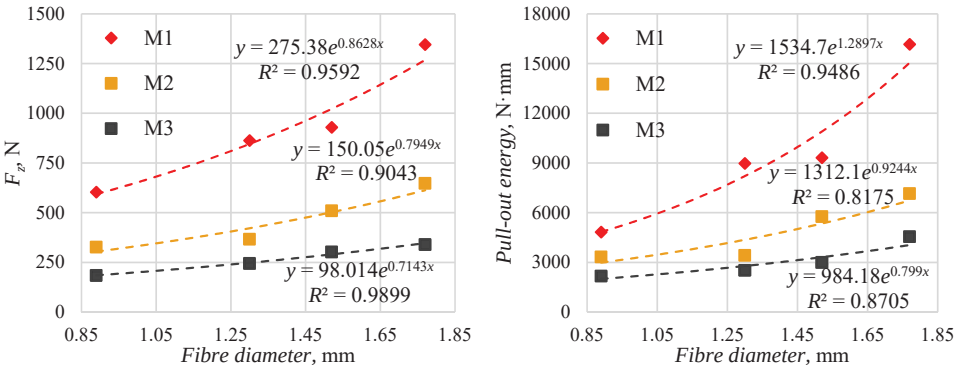

Fig. 2.19. Maximum pull-out force and energy depending on smooth composite fibre (CF1, CF1-A, CF1-B, and GF2) diameter in three concrete matrices: M1, M2, and M3.

Peak pull-out force and fibre diameter as well as fibre complete pull-out energy and fibre diameter are plotted in Fig. 2.19. From both figures it can be seen that there is clear relationship

(exponential) between the diameter and maximum fibre pull-out force as well as between the diameter and complete fibre pull-out energy.

Composite fibre shape and surface influence on single fibre pull-out

Three composite carbon fibres CF1, CF2, CF3 and composite glass fibre GF2 were selected to investigate different influence of shape and surface on single fibre pull-out behaviour from three concrete matrices. Pictures of fibres with extremely different shape and surfaces are presented in Fig. 2.20.

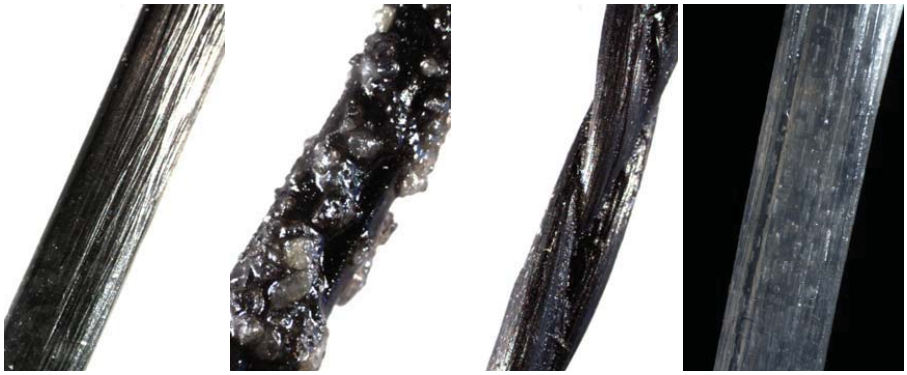

Fig. 2.20. Composite carbon and glass fibres with smooth surface, rough surface and braided shape: CF1, CF2, CF3, and GF2 (from the left).

Load rate influence on pull-out behaviour

Results with smooth composite carbon fibre CF1 show that load rate does not have a significant influence on single fibre pull-out behaviour in the range of 1–20 mm/min. The following assumption is made: fibre performance in fibre reinforced concrete (FRC) beams is similar to the one investigated during single fibre pull-out test. Therefore, single fibre pull-out behaviour and force-displacement curves can be used to explain the mechanics of fibre reinforced concrete.

Fibre failure modes

Single fibre pull-out or failure modes are discussed and fibre surface pictures before and after pull-out are presented in the subchapter of the Thesis. All single fibre pull-out tests are gathered in two main groups: pull-outs at different depths and 0-degree angle configuration to the testing force (group 1) and pull-outs at 15 mm or 25 mm embedment depth at 15–60-degree angle configuration (group 2). Fibre pull-out failure behaviour is discussed separately for group 1 and 2, but only distinctive fibre failure modes are described in the summary of the Thesis.

Pure fibre pull-out – this failure mode is observed mainly for composite fibres with a smooth surface and relatively thin outer epoxy layer. Fibre outer surface is without largely visible defects, but surface scratched are visible along the fibre longitudinal direction (CF1, CF1-A, CF1-B, CF3 in concrete matrices M2 and M3, GF2). Some fibre pull-out tests showed that fibre surface has a very light and “woolly” look due to the rubbing between fibre’s outer epoxy layer and concrete matrix channel. Friction in the interface layer deteriorates relatively soft epoxy resin layer (CF1-B in concrete matrix M2).

Fibre extraction from epoxy resin shell – this failure mode is observed for composite fibres with a rough surface and relatively thick epoxy and sand grain outer layer (CF2, CF2-A, CF2-B, GF3 in concrete matrix M3). Fibre outer layer normally is peeled off during the fibre pull-out process and the fibre has many surface defects. Normally fibre filaments have no defects and fibre strength is not affected. In this fibre failure mode, the weakest zone is the relatively thick epoxy layer. Part of the fibre outer layer as well as the shell is fastened in the concrete matrix and fibre motion is ensured by epoxy layer deformation and failure.

Fibre delamination and pull-out – this failure mode is mainly observed for composite fibres with a smooth surface at a 30–60-degree angle (CF1-B in concrete matrices M2 and M3). Fibre is delaminating during the pull-out due to defects in the fibre and large angle of configuration. Internal defects are mainly occurring due to a hand production process – fibre filaments are not completely impregnated with epoxy matrix. Fibres configured at a large angle are subjected to bending and therefore delamination risk is increased. Fibre filament delamination or separation in two or more fibre longitudinal parts causes significant pull-out resistance reduction and large deformations due to reduced fibre stiffness.

Fibre delamination and failure – this failure mode is observed for composite fibres with a smooth surface and large angle configuration (CF1-B in concrete matrix M2). Fibre delamination occurs due to the same reasons as in the case with fibre pull-out, but in this case, fibre fails due to rubbing along the concrete channel edge. The fibre being in the pull-out motion obtains additional defects due to the rubbing and these defects are arising along the fibre on one side. Fibre rupture occurs when a significant number of defects are accumulated and pull-out force exceeds the fibre tensile strength.

Fibre rupture – this fibre failure mode can be observed for composite fibres with a rough surface and smooth surface in concrete matrices with high strength (CF1-B in concrete matrix M1, CF2-B). Composite fibres with a rough surface are anchored enough and additional shear in the fibre due to angle configurations results in fibre rupture. The same happens with the smooth fibre in high strength concrete. The subchapter 5.4 of the Thesis explains that concrete matrix strength increases pull-out resistance and fibre anchorage for smooth fibres more compared to other composite fibre, therefore even smooth fibres at 15–60-degree angle configurations result in pure fibre rupture.

In **Chapter 6,** fibre reinforced beam flexural load bearing capacity is analysed.

Beam samples with composite fibres CF1, GF1, and GF2 (volume fraction V_f = 1.5 %) were manufactured to investigate fibre reinforced concrete behaviour in flexure. In order to evaluate and compare composite fibre performance with conventional fibres, reinforced concrete samples with straight (SF1) and corrugated steel fibres (SF2) were manufactured and tested as well. Concrete matrices M1, M2, and M3 were mixed according to the mixing procedure described in Chapter 2. A mix of 7 litres was prepared in each step, consistency was measured and samples for compressive strength were taken. Concrete beams with the size of 100 mm × 100 mm × 400 mm were cast in each mixing step. In total 4 beam samples were prepared for each fibre type and concrete matrix.

Fibre geometry and calculated dosage of kg per cubic meter are shown in Table 2.5. Composite fibres have smaller density compared to steel, in result composite fibres are

necessary 4.5–7 times less by weight with the same volume fraction. Composite fibres CF1, and GF1 are only 15% and GF2 – 22% of steel fibre weight when the dosage is the same – 1.5 % volume fraction. Fibres with lower density are more suitable for highly flowing concrete mixtures and are less likely to segregate in the mix. Fibre dosages with less weight have also smaller load impact on equipment when fibres are introduced in a concrete mixer, truck or during the concrete casting process.

The samples were tested in four-point bending. Load and deflection in middle span were measured. The testing was carried out with a load rate of 0.25 mm/min. Average force-deflection curves are shown in Fig. 2.21–Fig. 2.23.

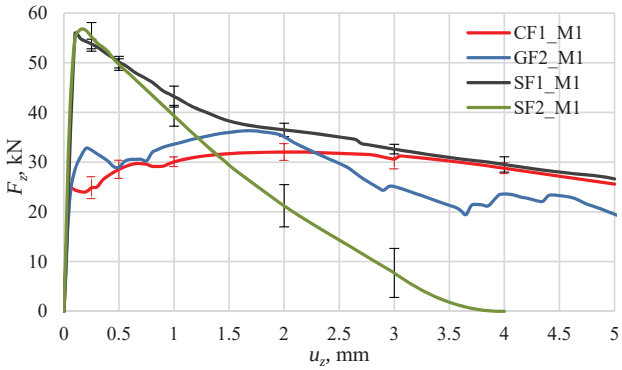

Fig. 2.21. Average load-deflection curves for beams (concrete matrix M1) subjected to bending: CF1, GF1, GF2, SF1, and SF4.

Composite carbon fibre (CF1) reinforced concrete shows strain hardening behaviour with 1.5 vol. fraction.

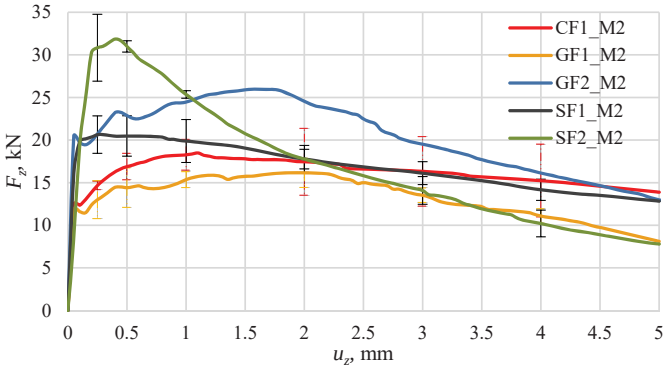

Fig. 2.22. Average load-deflection curves for beams (concrete matrix M2) subjected to bending: CF1, GF1, GF2, SF1, and SF2.

All three composite fibres show strain hardening behaviour in concrete matrix M2. Even though steel fibres increase concrete tensile strength, load gradually decreases after first crack occurrence for straight steel fibre SF1, and sharp decrease happens for SF2.

All tested fibre reinforced concrete (with M3 matrix) can be qualified as strain softening in bending, two fibres – GF4 and SF2 have fastest load decrease. These two fibre types have a

significant anchorage in concrete. SF2 has a high single fibre resistance during the pull-out, but composite fibre GF4 is not pulling out from concrete and failing.

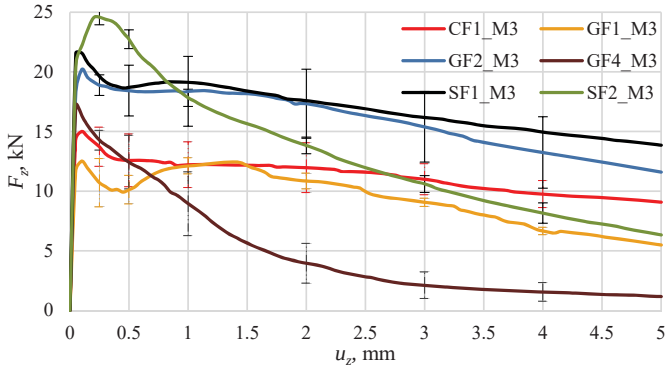

Fig. 2.23. Average load-deflection curves for beams (concrete matrix M3) subjected to bending: CF1, GF1, GF2, GF4, SF1, and SF2.

Fibre geometry (braided glass fibre filaments) and undulated surface produce significant anchorage. Fibres tensile strength is not balanced with anchorage in concrete matrix, therefore after the first crack in concrete beam sample, composite fibres gradually one after the other are rupturing and load-bearing capacity of the beam decreases sharply.

Table 2.5

Diameter, Dosage and Number of Fibres in the Crack Plane

Fibre type	Diameter, mm	L/d ratio	Dosage, kg/m^3	Fibre count, [number]				*L*/*d*
				M1	M2	M3	Average	
CF1	1.77	28.3	16.9	54.5	37.5	43.7	45.2	28.3
GF1	2.18	22.9	17.9	26.3	25.8	28.5	26.8	22.9
GF2	1.52	32.9	26.2	42.3	39.8	39.5	40.5	32.9
GF4	1.88	27.66	19.7	–	–	37	–	26.6
SF1	0.79	63.4	117	146	155	155	152	63.4
SF2	1.0	50	117	117	113	125	118.3	50

After performing a bending test, beam samples were separated completely to count fibres in the crack plane. From the Table 2.5, it can be seen that the number of composite fibres is significantly smaller than number of steel fibres. The number of fibres in a crack plane for composite CF1 and GF2 is approximately 3.5–3.8 times smaller compared to SF1. It is evident that higher *L*/*d* ratio results in a higher number of fibres in the crack plane. The number of fibres in crack plane showed a direct relation to bending behaviour. The samples with a larger fibre count in the crack showed higher load curve. A significant advantage of composite fibre GF2 is a small number of the fibres generating bending resistance through the fibre pull-out. A large number of fibres worsens concrete rheological properties and there are higher requirements for the mix flow properties and stability to be able to introduce high vol. fractions of the fibres.

3. CONCLUSIONS

1. Composite carbon and glass fibres, as well as hybrid fibres, were developed with a diameter in the range of 0.89–2.76 mm. Different manufacturing techniques were tested to achieve smooth and rough surfaces as well as undulated shape. Most appropriate industrial manufacturing technique was found, and a patent application filed; the technique allows producing smooth composite fibres with different diameters and length as well as a rough surface which is realised by sand grain application on the fibre outer surface. Braided fibres can also be manufactured in the industrial process due to relatively simple braiding process automatization.

2. Use of multi-walled carbon nanotubes (MWCNT) and carbon microfibres does not provide the expected performance; the experiments revealed that MWCNT are too small and carbon microfibres are too big to reinforce concrete hierarchically. There is a huge gap in fibre size between MWCNT and macrofibres and reinforcement is not efficient – microcracks in the fibre channel were observed in SEM images. Also, increase in single steel fibre pull-out resistance was insignificant and reached only 8 % peak pull-out force and pull-out energy for samples with combined MWCNT and carbon microfibres.

3. Straight steel fibre (SF1) pull-out resistance is very dependent on concrete matrix strength, this applies to all embedment depths. Single fibre pull-out peak force is double in concrete matrix M2 compared to M3, and in M1 compared to M2. Pull-out curves in concrete matrix M2 and M3 show an increase in curve's tail, which can be explained with plug formation from concrete dust and grains during the pull-out process and channel degradation. Pull-out force reduction during the pull-out process is slower in the concrete matrix with higher strength.

4. Corrugated steel fibre (SF2) in concrete matrix M1 has significant anchorage – 10, 15 mm embedment generates more than 700 N of maximum force. Fibres in concrete matrix M2 in 15–25 mm depth have almost the same peak pull-out force, but the most significant difference is post-peak between 10 and 15 mm of fibre displacement. All fibres extracted from concrete matrix M1 and M2 were straightened. Fibres in concrete matrix M3 had a slight influence from the embedment depth in the range of 15–25 mm because most of the fibres remained slightly corrugated – fibres were deformed and concrete channel was damaged (due to low strength).

5. Composite carbon and glass fibres with a smooth surface (CF1, CF1-A, CF1-B, and GF2) have steep force increase until fibre delamination occurs and moderate increase follows until the peak force is reached. Smooth composite fibres show almost linear force reduction after reaching the peak force in all embedment depth configurations. Smooth composite fibre peak pull-out force has a linear dependence on the embedment depth.

6. Composite carbon fibres with a rough surface (CF2, CF2-A, CF2-B) have steep force increase up to the peak pull-out force. Pull-out force reduction after the peak is very fast, which gradually becomes moderate. The results show that fibre, which is pulling out from the concrete matrix, fails in the outer layer of the fibre (fibre filament core is extracting from the shell with epoxy resin and grains, which produce surface roughness).

7. Composite carbon fibre CF3 with undulated shape and smooth surface show similar pull-out behaviour to CF2 fibre group. It has steep pull-out force increase until the peak and rapid decline after. However, force increase line until the peak does not allow to identify the fibre delamination point. This is related to fibre braided structure, which can have longitudinal deformations when it is stretched. Composite fibre is failing to pull-out at 20–25 mm embedment in concrete matrix M1; fibre in other matrices shows consistent fibre peak pull-out force dependence on embedment depth.

8. Composite fibres with smooth surface show high resistance to pull-out when fibres are configured at an angle of 15–30 degrees to the force. An angle of 15–30 degrees shows a significantly higher resistance to pull-out compared to 0-degree, a 45-degree angle shows similar or lower and 60-degree angle shows lower resistance. Fibres with a smaller diameter (CF1-B) show fibre rupture in most angle configurations in concrete matrix M1 due to low shear resistance. Fibre test results showed that internal fibre defects also influence resistance and are more subjected to fibre longitudinal delamination, therefore pull-out resistance is lower. Composite fibres with rough surface showed weak resistance in the pull-out process when configured at angles to the force.

9. Composite fibres with smooth surface showed significant pull-out resistance dependence on concrete matrix strength. Single fibre pull-out resistance is higher in the concrete matrix with a higher strength. Fibres CF1, CF1-A, and CF1-B have 1.85–2.35 times higher pull-out peak force in concrete matrix M1 compared to M2 and 1.5–1.9 times higher in M2 compared to M3. Composite fibres with rough surface have a pull-out dependence on matrix strength, but not so pronounced as smooth composite fibres. Composite fibre CF2 has 1.17–1.3 times higher pull-out peak force for concrete matrix M1 compared to M2 and for M2 compared to M3.

10. Composite fibres with smooth surface have an exponential relationship between the peak pull-out force and fibre diameter. A larger fibre diameter (in a range of 0.87–1.77 mm) provides a higher pull-out force. This relationship exists in all concrete matrices. However, a matrix with higher strength has a faster peak force growth when the fibre diameter is increased.

11. Composite fibre shape and surface have a pronounced influence on fibre pull-out behaviour. Smooth fibres have significantly lower peak force in all matrices compared to fibres with a rough surface, however, in concrete matrix M1, it shows highest pull-out energy for complete fibre extraction. Composite fibres with rough surface show the highest peak pull-out force in all three matrices, but complete fibre extraction energy is equal to fibre CF3 with an undulated shape in M2 and the highest among the fibres in concrete matrix M3. The composite fibres with smooth surface show better overall performance in concrete matrices with higher strength and fibres with a rough surface are more beneficial for concrete matrices with lower strength.

12. Five different fibre extraction and failure modes were observed: (1) pure fibre pull-out, (2) fibre delamination and pull-out, (3) fibre extraction from epoxy resin shell, (4) fibre delamination and failure, as well as (5) fibre rupture.

13. Fibre reinforced concrete beams show strain hardening behaviour in flexure with CF1, GF2 fibres and M1, M2 matrix. Concrete matrix M1 with glass fibre GF1 fails in a brittle

manner due to uneven fibre shape, which generates too high fibre anchorage in the concrete. All composite fibres have a very low L/d aspect ratio and fibre count in the crack plane (compared to steel fibres with the same vol. fraction).

14. Concrete matrix strength shows pronounced influence on FRC beam behaviour. High strength concrete matrices have to be reinforced with high strength fibres to achieve a reliable material with strain hardening properties; low strength concrete matrices have to be reinforced with engineered fibre surface that highly resists to the pull-out. Results for three concrete compressive strength matrices allow to interpolate intermediate results.

15. Fibre surface can be engineered to adjust the pull-out resistance to the fibre tensile strength and achieve the desired fibre reinforced concrete behaviour in tension and flexure.

4. LIST OF REFERENCES

1. Gettu, R., Gardner, D.R., Saldívar, H., Barragán, B.E. Study of the distribution and orientation of fibers in SFRC specimens. Materials and Structures/Materiaux et Constructions 38, 2005, 31–37.
2. Herrmann, H., Pastorelli, E., Kallonen, A., Suuronen, J. Methods for fibre orientation analysis of X-ray tomography images of steel fibre reinforced concrete (SFRC). Journal of Materials Science, 51(8), 2016, 3772–3783. doi:10.1007/s10853-015-9695-4
3. Eik, M., Puttonen, J., Herrmann, H. An orthotropic material model for steel fibre reinforced concrete based on the orientation distribution of fibres. Composite Structures, 121, 2015, 324-336. doi:10.1016/j.compstruct.2014.11.018
4. Péter, J. K. Determining the orientation of steel and synthetic fibres in fibre reinforced concrete. [Acél és szintetikus szálak orientációjának meghatározása szálerosítésu betonban] Epites-Epiteszettudomany, 46(1–2), 2018, 221-–238. doi:10.1556/096.2017.007
5. Zhang, S., Liao, L., Song, S., Zhang, C. Experimental and analytical study of the fibre distribution in SFRC: A comparison between image processing and the inductive test. Composite Structures, 188, 2018, 78–88. doi:10.1016/j.compstruct.2018.01.006
6. Kim, H., Kang, D., Oh, S. J., Joo, C. Nondestructive evaluation on dispersion of steel fibers in UHPC using THz electromagnetic waves. Construction and Building Materials, 172, 2018, 293–299. doi:10.1016/j.conbuildmat.2018.03.238
7. Lim, S., Raju, R. A., Matsuda, M., Okamoto, T., Akiyama, M. Structural behavior prediction of SFRC beams by a novel integrated approach of X-ray imaging and finite element method. Construction and Building Materials, 170, 2018, 347–365. doi:10.1016/j.conbuildmat.2018.03.079
8. Mínguez, J., González, D. C., Vicente, M. A. Fiber geometrical parameters of fiber-reinforced high strength concrete and their influence on the residual post-peak flexural tensile strength. Construction and Building Materials, 168, 2018, 906–922. doi:10.1016/j.conbuildmat.2018.02.095
9. Löfgren, I. and Gylltoft, K.: In-situ cast concrete building: Important aspects of industrialised construction, Nordic Concrete Research, 1/2001, pp. 61–80.
10. Beddar, M. Fibre-reinforced concrete: Past, present and future. Concrete (London), 38(4), 2004, 47–49.
11. Naaman, A., Wongtanakitcharoen, T. and Hauser, G., Influence of different fibers on plastic shrinkage cracking of concrete, ACI Mater J, Vol. 32, 2, 102–107, 2005.
12. Pereira, E.B., Fischer, G. and Barros, J.A.O., Direct assessment of tensile stress-crack opening behavior of Strain Hardening Cementitious Composites (SHCC). Cement and Concrete Research, 42, 2012, 834–846.
13. Pereira, E. B., Fischer, G., Barros, J. A. O. Direct assessment of tensile stress-crack opening behavior of strain hardening cementitious composites (SHCC). Cement and Concrete Research, 42(6), 2012, 834–846.
14. Fischer, G., Lárusson, L. H., Jönsson, J. Prefabricated floor and roof panels with engineered cementitious composites (ECC). Paper presented at the Proceedings of the 2009

Structures Congress – Don't Mess with Structural Engineers: Expanding our Role, 2009, 2199–2208. doi:10.1061/41031(341)241

15. Fischer, G. Application of engineered cementitious composites (ECC) in prefabricated modular housing. Paper presented at the American Concrete Institute, ACI Special Publication, (268 SP), 2006, 17–27.
16. Fischer, G., Li, V. C. Effect of fiber reinforcement on the response of structural members. Engineering Fracture Mechanics, 74(1–2), 2007, 258–272. doi: 10.1016/j.engfracmech. 2006.01.027
17. Sahmenko, G., Krasnikovs, A., Lukasenoks, A., Eiduks, M. "Ultra High Performance Concrete Reinforced with Short Steel and Carbon Fibers." In: Environment. Technology. Resources: Proceedings of the 10th International Scientific and Practical Conference, Latvia, Rezekne, June 18–20, 2015, 193–199.
18. Patnaik A., Miller L., Adhikari S., Standal P. C. Basalt FRP Minibar reinforced concrete, Fibre Concrete 2013, September 12–13, 2013, Prague, Czech Republic.
19. Patnaik A., Miller L., Standal P. C. Fiber reinforced concrete made from Basalt FRP Minibar, Proceedings of the 1st Concrete Innovation Conference (CIC), 11–13 June 2014, Oslo, Norway, ISBN 978-82-8208- 0415.
20. Tabatabaei, Z.S., Volz, J.S., Keener, D.I., and Gliha, B.P., Comparative Impact Behavior of Four Long Carbon Fiber Reinforced Concretes, Materials & Design, Vol. 55, March 2014, 212–223
21. Tabatabaei, Z. S., Volz, J. S., Baird, J., Gliha, B. P., Keener, D. I. Experimental and numerical analyses of long carbon fiber reinforced concrete panels exposed to blast loading. International Journal of Impact Engineering, 57, 2013, 70–80.
22. Tabatabaei, Z. S., Volz, J. S., Gliha, B. P., Keener, D. I. Development of long carbon fiber-reinforced concrete for dynamic strengthening. Journal of Materials in Civil Engineering, 25(10), 2013, 1446-1455. doi:10.1061/(ASCE)MT.1943-5533.0000692
23. Pupurs A., Krasņikovs A., Pakrastiņš L. Micro-mechanical stress-state analysis of fibre reinforced concrete (FRC), Scientific Proceedings of Riga Technical University (Architecture and Construction Science) – 7, 2006, 160.–171.
24. Krasnikovs A., Kononova O., Pupurs A. Steel Fiber Reinforced Concrete Strength. Sc. Proceedings of Riga Technical University. Transport and Engineering, 6. Vol.28, Riga, 2008, 142–150.
25. Krasņikovs A., Kononova O., Pupurs A. Micromechanical Investigation of Steel Fiber Reinforced High-Performance Concrete Post-Cracking Behavior, Proceedings of International scientific conference Fiber Concrete 2009, Prague, Czech Republic, 2009, 110–124.